

Hysteresis of Néel-line motion and effective width of 180° Bloch walls in bulk iron

U. Hartmann and H. H. Mende

Institut für Angewandte Physik, Universität Münster, Corrensstrasse 2/4, D-44 Münster, Federal Republic of Germany

(Received 18 November 1985; revised manuscript received 27 December 1985)

Subdivided 180° Bloch walls of alternating polarity have been observed on iron whiskers employing the interference-contrast colloid technique. The field-induced conversion of these complex walls is predominantly controlled by Néel-line motion. The static polarization curves, optically recorded for whiskers of various thicknesses, permit an experimental estimation of an effective Bloch-wall width which is in good agreement with the theoretically obtained value for bulk material.

Since the fundamental experimental work of De Blois and Graham,¹ iron whiskers with a Landau domain structure (see Fig. 1) are known to contain 180° Bloch walls of complex structure. The self-magnetostatic energy of these walls, which is due to free magnetic poles arising at the intersection of the wall with the surface of the crystal, causes the wall to divide into a periodic configuration of oppositely polarized wall segments.^{2,3} At the junction of two successive wall segments a Néel line (commonly called a Bloch line also, but it is preferable to reserve this second terminology for the analogous situation of a singularity in a Néel wall⁴) is located which provides a quasisubrupt change of the chirality, i.e., the handedness, of the wall (see Fig. 2). From a topological point of view these singularities have been considered as disclinations in the overall spin lattice.⁴

In the present study, the polarization reversal process of subdivided 180° Bloch walls in iron whiskers, under the influence of homogeneous magnetic fields applied parallel to the axis of wall polarization, i.e., parallel or antiparallel to the $[010]$ direction (see Fig. 2), is investigated under static conditions. *In situ* observations of field-dependent actual wall configurations are performed using the recently developed interference-contrast colloid (ICC) technique.⁵ In this magneto-optical technique the small stray-field-induced variations within the dielectric constant of a thin ferrofluid layer are transformed into contrast variations revealing details of the domain-wall fine structure invisible in the conventional Bitter technique. An analysis of the underlying complex contrast mechanism has been published elsewhere.^{6,7} Whiskers suitable for the observations are grown in a $\langle 100 \rangle$ direction and

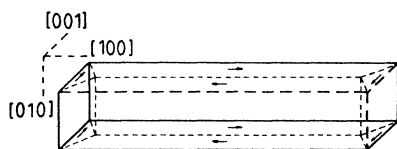


FIG. 1. Schematic sketch of a $\langle 100 \rangle$ -{100}-oriented iron whisker with a Landau domain structure.

bounded by optically perfect $\{100\}$ crystallographic faces. They have nearly square cross sections, 10 to $100 \mu\text{m}$ on a side, and a length ranging from 10 to 25 mm.

The alternating polarity of a subdivided wall is clearly revealed by the ICC technique when the whisker is subjected to a homogeneous vertical field generated by a pair of Helmholtz coils. As shown by Fig. 3, the colloid deposit on its surface is enhanced at wall segments polarized in the direction of the externally applied field and shifted

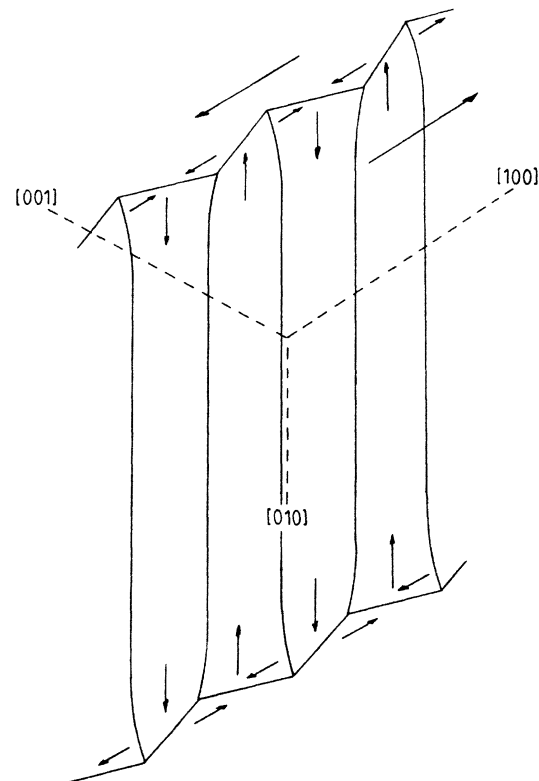


FIG. 2. Schematic illustration of the internal structure of a subdivided 180° Bloch wall in a whisker. The slight surface tilting of the individual segments causes a flux exchange between the wall and the adjacent domains (Ref. 3).

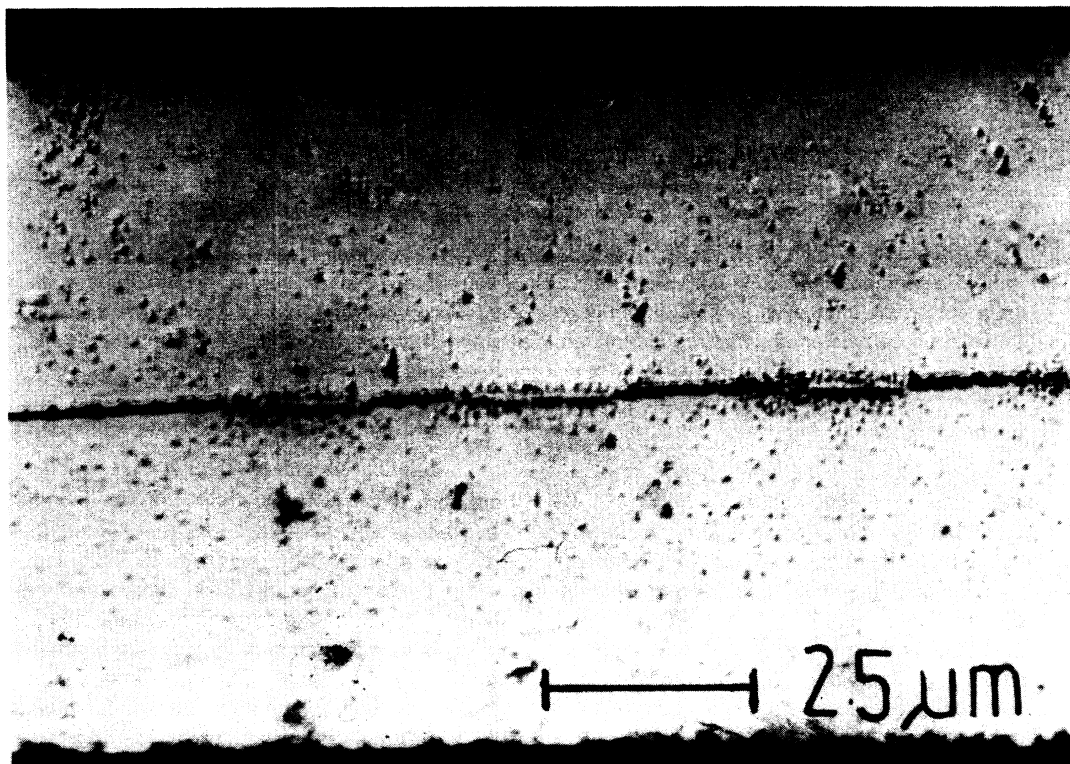


FIG. 3. ICC micrograph of a subdivided 180° Bloch wall under the influence of an externally applied homogeneous field of $H = 1.6 \text{ kA/m}$ (20 Oe) which is directed downward from the whisker surface.

from the oppositely polarized segments. For increasing field strength the former segments grow at the expense of the latter.

The successive measurement of the relative length of the individual segments dependent on the applied field yields the static polarization curve of the wall. Figure 4 shows a typical result obtained from a subdivided 180° Bloch wall of 9.5 mm length in a whisker of $30 \mu\text{m}$ thickness. Starting from the remanent state, the polarization curve of the wall changes linearly with field over a wide range. Simultaneous observation of the bottom and top faces of the whisker indicates that the Néel lines follow an

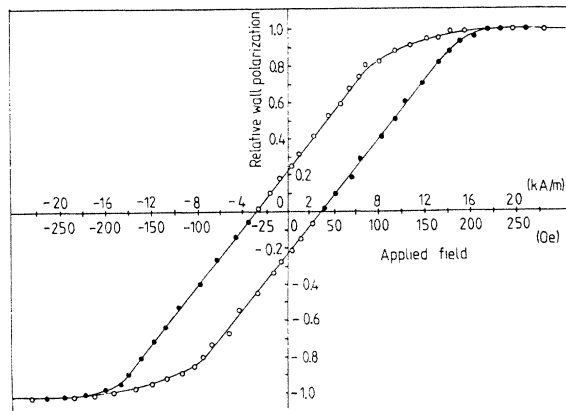


FIG. 4. Polarization curve of a subdivided 180° Bloch wall of 9.5 mm length in a whisker of $30 \mu\text{m}$ thickness recorded by ICC technique. The solid and the open circles correspond to increasing and decreasing field strength, respectively.

almost straight course through the whisker in this region. The suggested field-induced wall conversion is schematically illustrated by Fig. 5. Within the resolution of the Néel lines and thus the wall polarization is reversible up to an applied field of about 12 kA/m (200 Oe) (see Fig. 4). The approach to saturation is characterized by a decomposition of the vanishing segments into flux closure wall domains which exhibit a strong anchoring to some regions of the surface (see Fig. 6). During the occurrence of these triangular flux closure segments the obtained data only characterize the surface wall polarization which is a lower limit of the net wall polarization. No definitive information is obtained concerning the interior structure of the wall. The last closure segments disappear when a field of 18 kA/m (225 Oe) is reached (see Fig. 4). The resulting configuration corresponds to a relative wall polarization equal to unity. Upon decreasing the field from saturation, flux closure structures are observed to nucleate in various regions of the surface. Figure 7 shows the *in situ* observation of the nucleation process of a reverse wall segment at a small surface irregularity. The nuclei of reverse polarization exhibit a relatively gradual expansion with further decreasing field. At about 6 kA/m (75 Oe) all Néel lines at the top face of the whisker are observed to have their counterparts at the bottom face (see Fig. 4). Their field-induced motion is again reversible. The hysteresis of the polarization curve yields a relative remanence of 0.24 and a coercive field of 2.8 kA/m (35 Oe).

It should be noted that the Néel-line coercive field is much higher than the coercive field for the motion of the

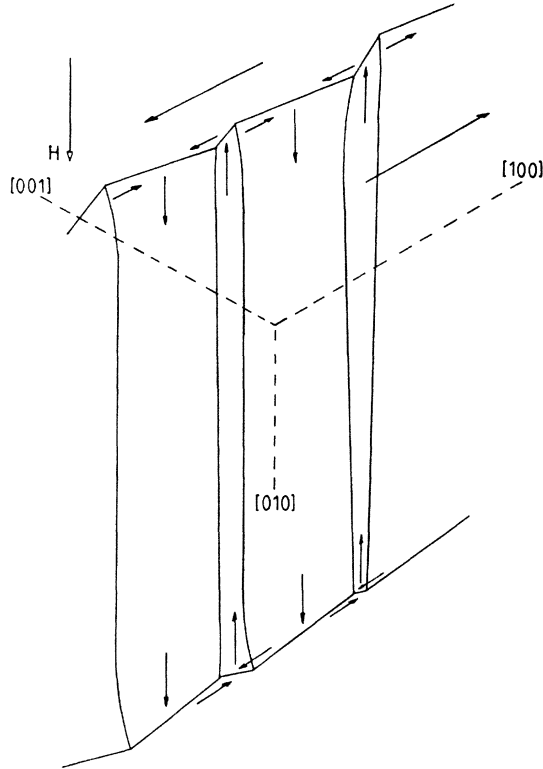


FIG. 5. Diagram of the suggested internal wall conversion under the influence of a vertical external field directed in the [010] direction.

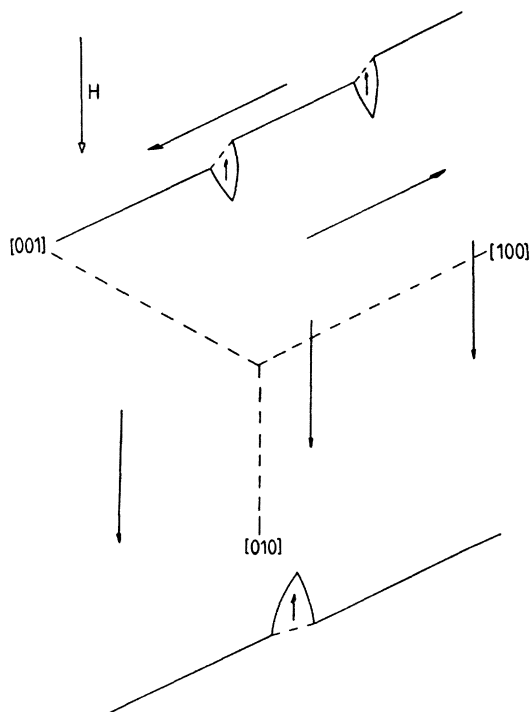


FIG. 6. Schematic drawing of the decomposition of vanishing wall segments into surface flux closure domains.

180° Bloch wall itself. The latter is of the order of 8 A/m (0.1 Oe) for an axial magnetization cycle of the whisker. A closer investigation of the wall polarization reversal process has established³ that the near perfection of some selected whiskers requires local wall nucleation fields, oriented antiparallel to the polarization direction of the previously fully saturated wall, which approach the theoretical coercive field limit resulting from magneto-crystalline anisotropy. The latter amounts to 44.8 kA/m (560 Oe) for iron at 25°C.⁸ On the other hand, conspicuous growth defects on the whisker surface are sources of high local demagnetizing fields and have been observed to be sites of easy wall nucleation (see Fig. 7). A slight decrease of the external field from saturation causes the formation of triangular flux closure segments (see Fig. 6) which then serve as nuclei of reverse polarization. Upon further decreasing external field the nuclei grow irreversibly until the reverse wall domains extend through the thickness of the whisker. Polarization reversal will then proceed easily by reversible movement of the Néel lines without any detectable hysteresis over the linear portion of the polarization curve in Fig. 4. Since the slope of the wall polarization curve near saturation is determined by surface flux closure effects, the observed coercive field of the wall depends critically upon the actual surface nucleation field contour of the whisker. On the other hand, recent investigations have confirmed³ that electropolishing of the whisker might serve to raise wall nucleation fields by smoothing out surface imperfections. For electropolished whiskers with a highly perfect surface, first measurements indicate a slight increase of the wall coercive field for increasing whisker thickness.³ Additionally, these measurements confirm that the slope of the wall polarization curve in the linear response region is fairly independent of the actual degree of surface perfection and only depends on the thickness of the whisker.

From the above results it follows that, due to the reversibility of the wall polarization reversal over the linear portion of the polarization curve in Fig. 4, complete depolarization of the subdivided wall, i.e., a configuration of zero wall polarization at zero field, cannot be achieved by application of a gradually decreasing ac field parallel to the axis of wall polarization. Satisfactory results are obtained by annealing of the whisker at temperatures above the Curie point which is 770°C for iron.

In the linear-response limit of the polarization curve the effective wall susceptibility χ_0 is defined by

$$\chi_0 = \frac{J_s}{\mu_0} \lim_{H \rightarrow H_c} \frac{\partial j}{\partial H}, \quad (1)$$

where J_s denotes the room-temperature saturation polarization of iron, H the applied magnetic field, H_c the Bloch-wall coercive field, and j the relative wall polarization ranging between 0 and 1. Due to the high interior crystallographic perfection of the whisker, the field-induced wall conversion is predominantly determined by the net inner demagnetizing field of the wall which is created by the free magnetic poles arising at the intersection with the surface. Within the linear-response region $\chi = \chi_0$ of the polarization curve in Fig. 4, the effective wall susceptibility χ is thus given by⁹

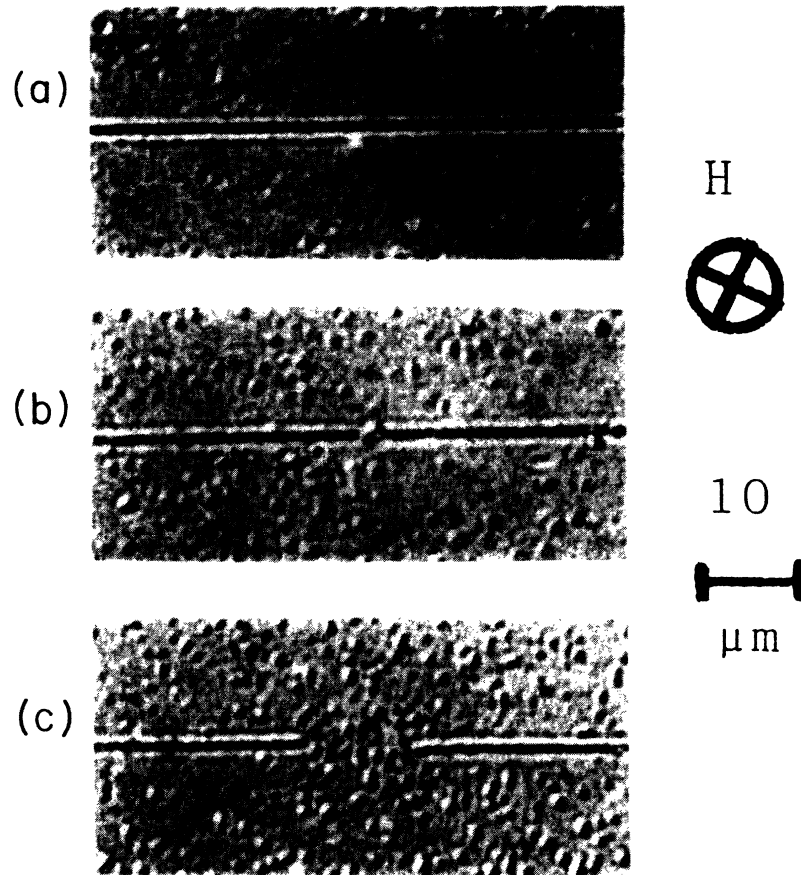


FIG. 7. *In situ* observation (ICC technique) of the nucleation of a reverse wall segment at a small surface irregularity [marked by the arrow in (a)] in decreasing external field directed downward for the whisker surface. The wall is completely saturated for $H = 18$ kA/m (225 Oe) in (a). In (b) the nucleus arises at the surface defect for $H = 16$ kA/m (200 Oe). The segment of reverse polarization exhibits a relatively gradual expansion with further decreasing field and is still of triangular flux closure shape for $H = 8$ kA/m (100 Oe) in (c).

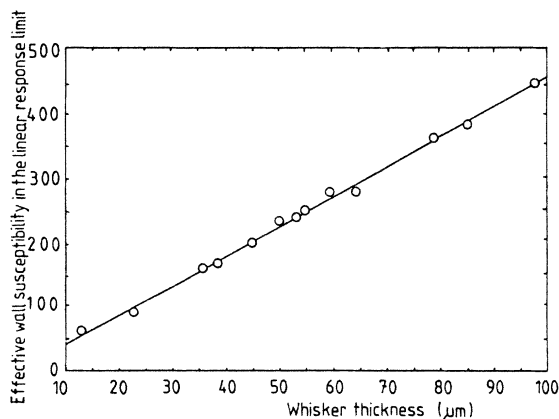


FIG. 8. Effective Bloch-wall susceptibility within the linear region of the polarization curve dependent on the whisker thickness. The indicated curve represents the least-squares fit.

$$\chi = N^{-1}, \quad (2)$$

where N is the effective geometrical depolarization coefficient of the 180° Bloch wall. The characterization of the inner demagnetizing field by a homogeneous effective depolarization coefficient is substantially equivalent to the classical approach of Néel¹⁰ in which the 180° spin transition is approximated by a homogeneous polarized cylinder of infinite length and with an elliptic cross section. The major axes of the cross section are determined by the wall width δ and the crystal thickness t . In a 180° Bloch wall the polarization is restricted to the longer axis t . The resulting geometrical depolarization coefficient is then given by

$$N = \delta t^{-1} \text{ with } \delta \ll t. \quad (3)$$

In order to check this result against experiment, the effective wall susceptibility has been measured according to Eq. (1) with $J_s = 2.16$ T (Ref. 11) for whiskers of various thicknesses. Figure 8 clearly confirms the linear depen-

dence of the wall susceptibility on the whisker thickness as expected from Eqs. (2) and (3) for the linear-response limit. According to this linearity, the obtained data permit an experimental estimation of the effective Bloch-wall width δ :

$$\delta = (\partial\chi/\partial t)^{-1}. \quad (4)$$

The computer fit from Fig. 8 yields a room-temperature value of $\delta = 228$ nm.

Following the calculations of Lilley,¹² the effective thickness of a {100} Bloch wall in a bulk crystal of iron should be given by

$$\delta_0 = 10.87 (A/K)^{1/2}. \quad (5)$$

Uncertainties concerning the exact value of δ_0 arise predominantly from the not-exactly-known exchange constant A of iron. Taking¹¹ $K = 4.2 \times 10^4$ J/m³ for the magnetocrystalline anisotropy constant and $A = 1.43 \times 10^{-11}$ J/m, the effective wall width according to Eq. (5) is given by $\delta_0 = 200$ nm. This value agrees surprisingly well with the experimental result.

For the future it is hoped that a closer investigation of the wall polarization curve in the region near to wall saturation will provide more details of the actual spin configuration in the surface region and of resulting nucleation phenomena during the polarization process.

Financial support of the Deutsche Forschungsgemeinschaft is gratefully acknowledged.

¹R. W. de Blois and C. D. Graham, Jr., *J. Appl. Phys.* **29**, 932 (1958).

²S. Shtrikman and D. Treves, *J. Appl. Phys.* **31**, 147S (1960).

³U. Hartmann and H. H. Mende (unpublished).

⁴M. Kléman, *Phys. Rev. B* **13**, 3091 (1976).

⁵U. Hartmann and H. H. Mende, *J. Phys. D* **18**, 2285 (1985).

⁶U. Hartmann and H. H. Mende, *J. Phys. (Paris) Colloq.* **46**, C6-279 (1985).

⁷U. Hartmann and H. H. Mende, *Z. Phys. B* **61**, 29 (1985).

⁸W. F. Brown, Jr., *Rev. Mod. Phys.* **17**, 15 (1945).

⁹R. M. Bozorth, *Ferromagnetism*, 2nd ed. (Van Nostrand, Toronto, 1953).

¹⁰L. Néel, *C. R. Acad. Sci. Paris* **241**, 533 (1955).

¹¹Landolt-Börnstein, *Zahlenwerte und Funktionen*, 6th ed. (Springer, Berlin, 1962), Vol. II. 9I.

¹²B. A. Lilley, *Philos. Mag.* **41**, 792 (1950).

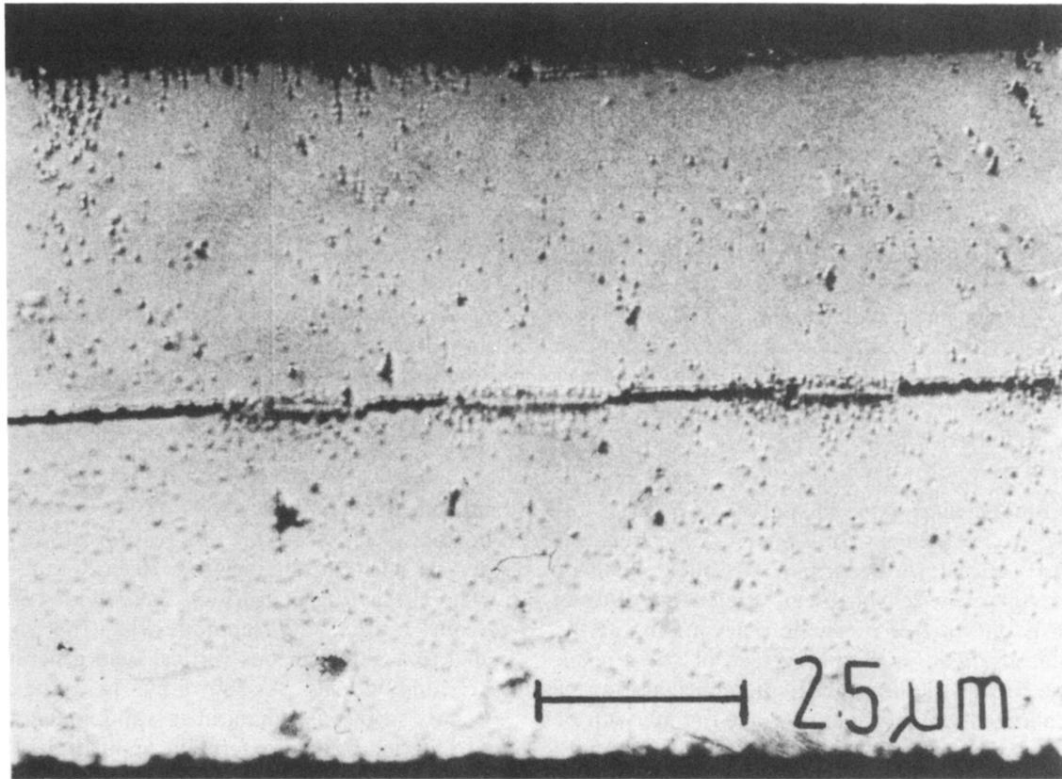


FIG. 3. ICC micrograph of a subdivided 180° Bloch wall under the influence of an externally applied homogeneous field of $H = 1.6 \text{ kA/m}$ (20 Oe) which is directed downward from the whisker surface.

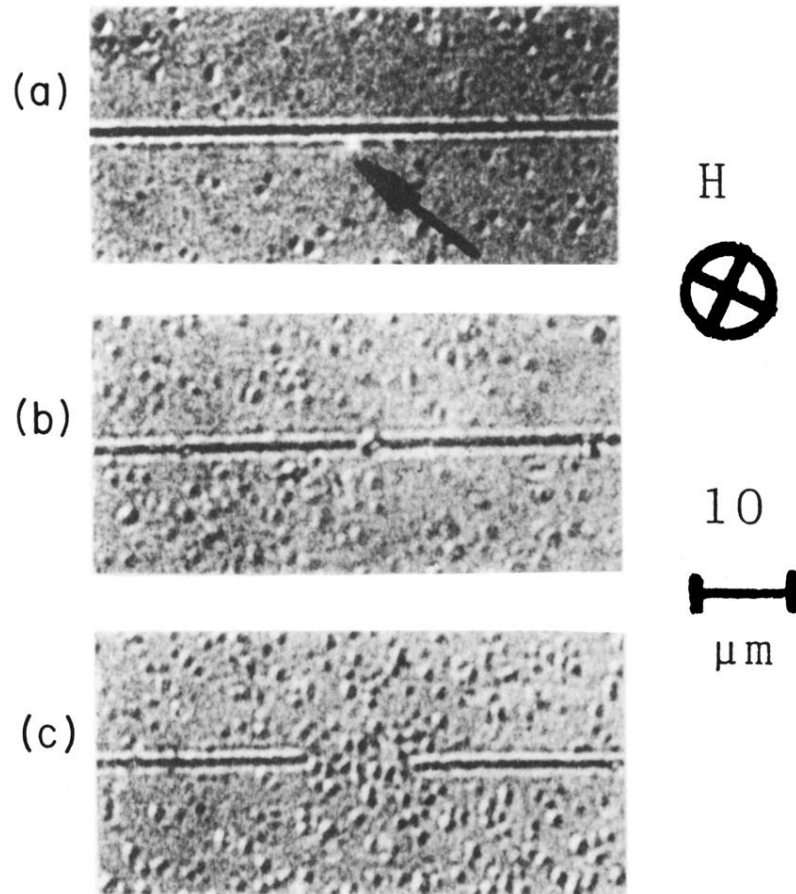


FIG. 7. *In situ* observation (ICC technique) of the nucleation of a reverse wall segment at a small surface irregularity [marked by the arrow in (a)] in decreasing external field directed downward from the whisker surface. The wall is completely saturated for $H = 18 \text{ kA/m}$ (225 Oe) in (a). In (b) the nucleus arises at the surface defect for $H = 16 \text{ kA/m}$ (200 Oe). The segment of reverse polarization exhibits a relatively gradual expansion with further decreasing field and is still of triangular flux closure shape for $H = 8 \text{ kA/m}$ (100 Oe) in (c).